



This is a repository copy of *Non-coherent DOA estimation via proximal gradient based on a dual-array structure*.

White Rose Research Online URL for this paper:  
<http://eprints.whiterose.ac.uk/171397/>

Version: Published Version

---

**Article:**

Wan, Z. and Liu, W. [orcid.org/0000-0003-2968-2888](https://orcid.org/0000-0003-2968-2888) (2021) Non-coherent DOA estimation via proximal gradient based on a dual-array structure. *IEEE Access*, 9. pp. 26792-26801. ISSN 2169-3536

<https://doi.org/10.1109/access.2021.3058000>

---

**Reuse**

This article is distributed under the terms of the Creative Commons Attribution (CC BY) licence. This licence allows you to distribute, remix, tweak, and build upon the work, even commercially, as long as you credit the authors for the original work. More information and the full terms of the licence here:  
<https://creativecommons.org/licenses/>

**Takedown**

If you consider content in White Rose Research Online to be in breach of UK law, please notify us by emailing [eprints@whiterose.ac.uk](mailto:eprints@whiterose.ac.uk) including the URL of the record and the reason for the withdrawal request.



[eprints@whiterose.ac.uk](mailto:eprints@whiterose.ac.uk)  
<https://eprints.whiterose.ac.uk/>

Received December 28, 2020, accepted February 2, 2021, date of publication February 8, 2021, date of current version February 17, 2021.

Digital Object Identifier 10.1109/ACCESS.2021.3058000

# Non-Coherent DOA Estimation via Proximal Gradient Based on a Dual-Array Structure

ZHENGYU WAN AND WEI LIU<sup>1</sup>, (Senior Member, IEEE)

Department of Electronic and Electrical Engineering, The University of Sheffield, Sheffield S1 3JD, U.K.

Corresponding author: Wei Liu (w.liu@sheffield.ac.uk)

This work was supported by the U.K. Engineering and Physical Sciences Research Council (EPSRC) under Grant EP/T517215/1.

**ABSTRACT** Although the non-coherent direction of arrival (DOA) estimation problem can be solved by sparse phase retrieval algorithms, known reference signals are required to deal with the inherent ambiguity issue of this approach. To avoid the use of reference signals, an effective array structure employing two uniform linear arrays is proposed (although other array structures are possible, such as the circular array), based on which a phase retrieval problem employing group sparsity is formulated. It is then replaced by its convex surrogate alternative by applying the majorization-minimization technique and the proximal gradient method is employed to solve the surrogate problem. The proposed algorithm is referred to as fast Group sparsity Based phase Retrieval (ToyBar). Unlike the existing phase-retrieval based DOA estimation algorithm GESPAR, it does not need to know the number of incident signals in advance. Simulation results indicate that the proposed algorithm has a fast convergence speed and a better estimation performance is achieved.

**INDEX TERMS** DOA estimation, phase retrieval, group sparsity, dual-arrays, majorization-minimization, proximal gradient.

## I. INTRODUCTION

Direction of arrival (DOA) estimation has various applications such as radar, sonar and wireless communications [1]. Traditionally, the phase information is assumed to be available at the array of sensors and many proposed high resolution DOA estimation algorithms often rely on this assumption, such as MUSIC [2], ESPRIT [3] and those based on compressive sensing [4]–[6]. However, in real applications, the phase information may not be reliable due to various reasons and in the extreme case, we may only have the magnitude information.

For such a non-coherent DOA estimation problem, a sparse phase retrieval algorithm called GESPAR is modified to solve it [7], [8], where the inherent ambiguity issue of non-coherent measurements was resolved using a reference signal when only one unknown source impinges upon the array. With more unknown signals, more reference signals are required. To reduce the number of required reference signals to one for multiple incident signals in [9], a method was proposed to firstly estimate the frequency component of non-coherent measurements, and then a high gain refer-

ence signal (12 dB over unknown signals) is employed to identify the DOA of unknown signals. Alternatively, with a normal gain reference signal, a dual-array structure was proposed to reduce the number of required reference signals to one in [9], but its estimation accuracy relies on its frequency resolution, which requires a large number of measurements. In addition, this method fails to utilize the information of multiple snapshots jointly to improve its performance. In [10], it was proved that the gap between non-coherent and coherent DOA estimation would be small if the number of sensors is large and then it employed a sparse phase retrieval algorithm called Phaselift to find the direction from non-coherent measurements. An approximation expression of Cramér-Rao bound (CRB) of non-coherent DOA estimation for one unknown incident signal by assuming a large gain reference signal was presented in [11], [12].

All the aforementioned methods require at least one reference signal at one end of the interested angle area with precisely known DOA in order to remove the ambiguities arising from non-coherent measurements, which is a challenge in practical operations [13], [14].

In this paper, firstly the ambiguities related to non-coherent measurements are revisited. Apart from the well-known

The associate editor coordinating the review of this manuscript and approving it for publication was Hasan S. Mir.

mirroring and spatial shift ambiguities, a new ambiguity issue called spatial order ambiguity is identified for the first time and discussed in detail and a solution to avoid this ambiguity is to limit the inter-sensor spacing of the employed uniform linear arrays (ULAs) to be less than a quarter of the signal wavelength for the normal DOA range of  $[-90^\circ, 90^\circ]$ . This is consistent with previous observation that with the standard half-wavelength spacing, the DOA range of the signals is limited to either  $[0, 90^\circ]$  or  $[-90^\circ, 0]$ . Secondly, to avoid the mirroring and spatial shift ambiguities, a dual-array structure without the need of any reference signals for multiple impinging sources is proposed with a detailed derivation to show its working. In essence, it utilizes the non-linear property of the sinusoidal function, and a unique DOA result is guaranteed with two sets of sinusoidal difference values. This part of the work was partially presented in our earlier conference paper [15]. Compared to [15], the mirroring ambiguity in the estimation process is solved in a different way in this version to explain the separate estimation method more clearly.

Thirdly, the non-coherent DOA estimation problem based on the proposed dual-array structure is represented as a joint group sparsity phase retrieval problem. The idea of phase retrieval via majorizaion-minimization technique (PRIME) [16] is then employed to formulate the problem as a group Least Absolute Shrinkage and Selection Operator (LASSO) problem, which can be solved by the proximal gradient. Nesterov acceleration is further implemented to improve the proposed algorithm. We refer to this algorithm as Fast jOint Group Sparse PhAsE Retrieval (ToyBar). With the proposed dual-array structure and the ToyBar algorithm, no reference signals are required when there are more than one incident signals; a reference signal is required in the scenario with only one incident signal, but the DOA of the reference signal can be arbitrary and unknown to the estimator.

The remaining part of the paper is structured as follows. Sec. II introduces the non-coherent signal model and the ambiguities of non-coherent measurements. Detailed analysis of the proposed dual-array structure for avoiding the mirroring and spatial shift ambiguities is presented in Section III. The proposed ToyBar algorithm is given in Section IV. Simulation results are provided in Sec. IV and conclusions are drawn in Sec. V.

## II. SIGNAL MODEL WITH TWO LINEAR ARRAYS

### A. DATA MODEL

The proposed array structure consists of two ULAs with an adjacent sensor spacing  $d$  as shown in Fig. 1, where the second array has a known angle  $\theta$  to the first one. The area of interest  $[-90^\circ, 90^\circ]$  is considered with respect to the broadside of each array. The number of sensors of the first array is  $N$ , while the second is  $M$  and since one sensor is shared between them, there are  $M + N - 1$  sensors in total.

Assume that there are  $K$  narrowband signals  $s_k$  with the same wavelength  $\lambda$  impinging from directions  $\theta_k$ ,  $k = 1, 2, \dots, K$ , respectively. The two corresponding

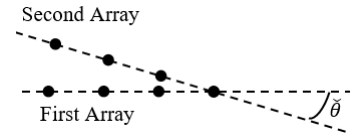


FIGURE 1. The dual-array structure with a shared sensor.

received signal vectors at time index  $p$  are expressed as

$$\begin{aligned} \mathbf{x}_1[p] &= \mathbf{A}_1(\theta)\mathbf{s}[p], \\ \mathbf{x}_2[p] &= \mathbf{A}_2(\theta)\mathbf{s}[p], \end{aligned} \quad (1)$$

where  $p = 1, \dots, P$  and  $\mathbf{x}_1[p] = [x_{1,1}[p], \dots, x_{N,1}[p]]^T \in \mathbb{C}^{N \times 1}$  and  $\mathbf{x}_2[p] = [x_{1,2}[p], \dots, x_{M,2}[p]]^T \in \mathbb{C}^{M \times 1}$  are measurements at first and second sub-arrays separately.  $\mathbf{s}[p]$  is the source signal vector expressed as

$$\mathbf{s}[p] = [s_1[p], s_2[p], \dots, s_K[p]]^T, \quad (2)$$

$\mathbf{A}_1(\theta)$  and  $\mathbf{A}_2(\theta)$  are steering matrices of the first and the second arrays, respectively. Their columns,  $\mathbf{A}_1(\theta_{k,1})$  and  $\mathbf{A}_2(\theta_{k,2})$ , for  $k = 1, \dots, K$ , are the corresponding steering vectors,

$$\begin{aligned} \mathbf{A}_1(\theta_{k,1}) &= [1, e^{-j2\pi \frac{d}{\lambda}(\sin \theta_{k,1})}, \dots, e^{-j(N-1)2\pi \frac{d}{\lambda}(\sin \theta_{k,1})}]^T, \\ \mathbf{A}_2(\theta_{k,2}) &= [1, e^{-j2\pi \frac{d}{\lambda}(\sin \theta_{k,2})}, \dots, e^{-j(M-1)2\pi \frac{d}{\lambda}(\sin \theta_{k,2})}]^T, \end{aligned} \quad (3)$$

where  $\theta_{k,1}$  and  $\theta_{k,2}$  are arriving angle of the  $k_{th}$  signal with respect to the broadside of the first and second arrays respectively. For noisy non-coherent measurements, we use the following data model

$$\begin{aligned} \mathbf{y}_1[p] &= |\mathbf{A}_1(\theta)\mathbf{s}[p]| + \mathbf{n}_1 \\ \mathbf{y}_2[p] &= |\mathbf{A}_2(\theta)\mathbf{s}[p]| + \mathbf{n}_2, \end{aligned} \quad (4)$$

where  $\mathbf{n}_1$  and  $\mathbf{n}_2$  are random Gaussian noise vectors, while  $|\cdot|$  is the element-wise absolute value operation.

### B. AMBIGUITIES

Reconstructing signals from (4) suffers from three ambiguities [17] and two of them would affect the DOA estimation results: one is mirroring and the other is spatial shift.

For mirroring, it refers to the phenomenon that the conjugated version of the original sources from the angles  $[-\theta_1, \dots, -\theta_K]$  will generate a set of measurements with the same magnitude as the original sources from  $[\theta_1, \dots, \theta_K]$ .

For the spatial shift ambiguity, it refers to the case that the received array signals are phase shifted by an unknown amount  $\phi$  as follows

$$\check{x}_n = e^{-jn\phi} x_n = \sum_{k=1}^K s_k e^{-jn\alpha \sin(\theta_k)} e^{-jn\phi}, \quad (5)$$

where  $x_n$  is the measurement at the  $n - th$  sensor with  $n = [0, \dots, N - 1]$ ,  $\alpha = 2\pi \frac{d}{\lambda}$ , the time index  $p$  has been dropped for convenience, and the effect of noise has been ignored. In this case, with the same set of source signals, a set of DOA angles,  $\check{\theta}_k$  satisfying  $\sin \check{\theta}_k = \sin \theta_k + \frac{\phi}{\alpha}$  for all  $k$ , would generate the same magnitude-only measurements.

One interesting property of this ambiguity is that, the DOA angle order stays the same, i.e. with  $\sin \theta_1 < \sin \theta_2 < \dots < \sin \theta_K$ , we also have  $\sin \check{\theta}_1 < \sin \check{\theta}_2 < \dots < \sin \check{\theta}_K$  and this ambiguity will not affect the relevant sinusoidal distance  $\Delta s_{\theta, kk'} = (\sin \theta_k + \frac{\phi}{\alpha}) - (\sin \theta_{k'} + \frac{\phi}{\alpha})$ ,  $k \neq k'$  due to the common phase shift involved for all DOA angles. As a result, with magnitude-only measurements, only the sinusoidal difference  $\Delta s_{\theta, kk'}$  can be measured.

However, there is another ambiguity which has not been discussed in literature yet and we call it ‘‘spatial order ambiguity’’, as this ambiguity will change the spatial order of the impinging signals, i.e. with  $\sin \theta_1 < \sin \theta_2 < \dots < \sin \theta_K$  we cannot have  $\sin \check{\theta}_1 < \sin \check{\theta}_2 < \dots < \sin \check{\theta}_K$ . Next, we discuss it in detail and show that this ambiguity can be avoided by limiting the adjacent sensor spacing to  $\lambda/4$ .

For this new ambiguity problem, we consider the following measurement with the same magnitude as  $x_n$  in (5)

$$\begin{aligned} \check{x}_n &= e^{-jn\phi} \sum_{k=1}^K s_k e^{-jn2\pi b_k} e^{-jn\alpha \sin \theta_k} \\ &= \sum_{k=1}^K s_k e^{-jn\alpha(\sin \theta_k + \frac{\phi}{\alpha} + \frac{b_k \lambda}{d})}, \end{aligned} \quad (6)$$

where  $b_k$  is an arbitrary integer. To avoid spatial aliasing, normally we assume  $d = \lambda/2$ . Then, (6) becomes

$$\check{x}_n = \sum_{k=1}^K s_k e^{-jn\alpha(\sin \theta_k + \frac{\phi}{\alpha} + 2b_k)}. \quad (7)$$

Without the  $b_k$  term, the maximum value of  $\frac{\phi}{\alpha}$  which can give a valid shift will be 2, i.e. shifting a signal from  $-90^\circ$  to  $90^\circ$ ; if it is larger than 2, the new shifted value will be larger than 1, which is not valid for  $\sin \theta$ . Similarly, the minimum value for  $\frac{\phi}{\alpha}$  will be  $-2$  and as a result we would have  $-2 \leq \frac{\phi}{\alpha} \leq 2$ .

Consider the original DOA angles are ordered as  $\sin \theta_1 < \sin \theta_2 < \dots < \sin \theta_K$  and with a shift by  $-2 \leq \frac{\phi}{\alpha} < 0$ , some of the DOA angles, such as  $\sin \theta_g, g = 1, \dots, G (G < K)$  are shifted to the left outside of the valid sinusoidal range so that  $\sin \theta_k + \frac{\phi}{\alpha} < -1$ , for  $k \leq G$ , while for the remaining angles, we still have  $-1 \leq \sin \theta_k + \frac{\phi}{\alpha} \leq 1$ ; then, we can choose  $b_k = 0$  for  $G < k \leq K$  and  $b_k = 1$  for  $k \leq G$ . As a result, we would have  $-1 \leq (\sin \theta_k + \frac{\phi}{\alpha} + 2b_k) \leq 1$  for  $k \leq G$ , which is valid angle values. However, in this case, we can see that the order of the new set of angles  $\check{\theta}_k$ , satisfying  $\sin \check{\theta}_k = \sin \theta_k + \frac{\phi}{\alpha} + 2b_k$  for all  $k$  will be different from the original one, i.e. we will not have  $\sin \check{\theta}_1 < \sin \check{\theta}_2 < \dots < \sin \check{\theta}_K$  any more and the sinusoidal difference of the original signals has changed. The net result is that the first  $G$  signals are shifted to the right side of the valid angle range, while the remaining signals are shifted to the left.

For example, consider  $K = 2$  signals with  $\theta_1 = -30^\circ$ ,  $\theta_2 = 90^\circ$  and  $\frac{\phi}{\alpha} = -2$ . After this shift,  $\sin \check{\theta}_2 = \sin \theta_2 - 2 = -1$  and  $\sin \check{\theta}_1 = \sin \theta_1 - 2 = -2.5$ . Obviously,  $\theta_2$  is shifted to  $-90^\circ$  and  $\check{\theta}_1$  does not exist. However, with half wavelength spacing,  $b_1$  can be chosen as 1, which leads to  $\sin \check{\theta}_1 = \sin \theta_1 - 2 + \frac{\lambda}{d} = -0.5$ . As a result, the solution is

$\check{\theta}_2 = -90^\circ$  and  $\check{\theta}_1 = -30^\circ$ . It can be seen that the order of DOA has changed as  $\sin \check{\theta}_2 < \sin \check{\theta}_1$  as well as the sinusoidal difference (from  $\Delta s_{\theta, 21} = 1.5$  to  $\Delta \check{s}_{\theta, 21} = 0.5$ ), but they still share the same magnitude measurement.

We have a similar conclusion if we consider the shift to the left with  $0 < \frac{\phi}{\alpha} \leq 2$ . This ambiguity cannot be solved by adding reference signals as the spacing in sine value among the new set of DOA angles will be different.

However, it can be resolved by reducing inter-sensor spacing  $d$  to  $d \leq \frac{\lambda}{4}$ . In the limit, we choose  $d = \frac{\lambda}{4}$ . Then

$$\check{x}_n = \sum_{k=1}^K s_k e^{-jn2\pi b_k} e^{-jn\alpha(\sin \theta_k + \frac{\phi}{\alpha} + 4b_k)}. \quad (8)$$

With  $-2 \leq \frac{\phi}{\alpha} \leq 2$ , for any value of  $b_k \neq 0$ , we always have

$$|\sin \theta_k + \frac{\phi}{\alpha} + 4b_k| > 1, \quad (9)$$

which means it is not a valid choice for any physical DOA angle. As a result, we can only have  $b_k = 0$ , i.e. we have avoided the spatial order ambiguity. Note here, we have assumed  $-2 \leq \frac{\phi}{\alpha} \leq 2$ , but  $\frac{\phi}{\alpha}$  can take any value outside this range; however, if it does take a value outside this range, it will be reduced to within this range by choosing an appropriate integer value for  $b_k$  in  $4b_k$ .

Therefore, in order to avoid this ambiguity,  $d$  is now chosen to be less than or equal to  $\lambda/4$  instead of  $\lambda/2$  for the normal angle range of interest  $[-90^\circ, 90^\circ]$ .

### III. PROPOSED DOA ESTIMATION METHODS

In this section, based on the dual-array structure, one method is presented first by estimating the set of DOAs relative to each subarray, which also shows that the dual-array structure is capable of solving the inherent shift and mirroring ambiguities. Then, a more effective joint group sparsity based DOA estimation method is proposed.

#### A. SEPARATE ESTIMATION METHOD

With the specific array structure, the area to be estimated for the first array is set as  $[-90^\circ + \check{\theta}, 90^\circ]$  while for the second array it is  $[-90^\circ, 90^\circ - \check{\theta}]$ , i.e. the common angle range of interest of both arrays, which is then uniformly divided into  $G (G \gg K)$  grid points and two corresponding overcomplete steering matrices  $\tilde{\mathbf{A}}_1$  and  $\tilde{\mathbf{A}}_2$  are constructed with each column representing a steering vector of a potential incident angle

$$\begin{aligned} \tilde{\mathbf{A}}_1 &= [\mathbf{a}(-90^\circ + \check{\theta}), \dots, \mathbf{a}(90^\circ)], \\ \tilde{\mathbf{A}}_2 &= [\mathbf{a}(-90^\circ), \dots, \mathbf{a}(90^\circ - \check{\theta})], \end{aligned} \quad (10)$$

Accordingly, the signal vector  $\mathbf{s}[p]$  is replaced by two  $G \times 1$  sparse vectors  $\tilde{\mathbf{s}}_1[p] = [s_{1,1}[p], \dots, s_{G,1}[p]]^T$  and  $\tilde{\mathbf{s}}_2 = [s_{1,2}[p], \dots, s_{G,2}[p]]^T$ , where only  $K$  entries at the corresponding incident angles are supposed to be non-zero. For the multiple-snapshot case, measurements of both arrays are expressed as  $\mathbf{Y}_1 = [\mathbf{y}_1[1], \dots, \mathbf{y}_1[P]]$  and  $\mathbf{Y}_2 = [\mathbf{y}_2[1], \dots, \mathbf{y}_2[P]]$ , where  $P$  is the number

of snapshots. Signal matrices are defined as  $\tilde{\mathbf{S}}_1 = [\tilde{\mathbf{s}}_1[1], \dots, \tilde{\mathbf{s}}_1[P]]$  and  $\tilde{\mathbf{S}}_2 = [\tilde{\mathbf{s}}_2[1], \dots, \tilde{\mathbf{s}}_2[P]]$ , and they can be reconstructed by

$$\begin{aligned} \min_{\tilde{\mathbf{S}}_1} \|\mathbf{Y}_1 - |\tilde{\mathbf{A}}_1 \tilde{\mathbf{S}}_1\|_F^2, \quad s.t. \|\tilde{\mathbf{S}}_1[p]\|_{2,0} \leq K, \\ \min_{\tilde{\mathbf{S}}_2} \|\mathbf{Y}_2 - |\tilde{\mathbf{A}}_2 \tilde{\mathbf{S}}_2\|_F^2, \quad s.t. \|\tilde{\mathbf{S}}_2[p]\|_{2,0} \leq K, \end{aligned} \quad (11)$$

where  $K$ ,  $\|\cdot\|_{2,0}$  and  $\|\cdot\|_F$  represents the number of incident signals,  $l_{2,0}$  norm and Frobenius norm, respectively. For the  $l_{2,0}$  norm of a matrix, it take the  $l_2$  norm of its row vectors, then form a new column vector, and finally take the  $l_0$  norm of the new column vector.

The above problem can be solved by applying the modified GESPAR algorithm [7] or the ToyBar algorithm proposed in the next section to each subarray individually. By solving the problem, the sinusoidal difference of all impinging signals of the first sub-array  $\Delta s_{\theta, kk', 1} = \sin \theta_{k, 1} - \sin \theta_{k', 1}$  and the second sub-array  $\Delta s_{\theta, kk', 2} = \sin \theta_{k, 2} - \sin \theta_{k', 2}$  are then obtained; however, they suffer from ambiguities as described in Section II-B and true DOAs cannot be found directly. The sinusoidal differences between smallest and largest incident signals impinging on the first and second arrays,  $\Delta s_{\theta, max, 1}$  and  $\Delta s_{\theta, max, 2}$ , have the following relationship with the four real DOA angles  $\theta_{K, 1}$ ,  $\theta_{1, 1}$ ,  $\theta_{K, 2}$ ,  $\theta_{1, 2}$

$$\begin{aligned} \Delta s_{\theta, max, 1} &= \sin(\theta_{K, 1}) - \sin(\theta_{1, 1}), \\ \Delta s_{\theta, max, 2} &= \sin(\theta_{K, 2}) - \sin(\theta_{1, 2}) \end{aligned} \quad (12)$$

One condition for the above equations is that angle range of the signals of interest of the first array should be limited between  $-90^\circ + \check{\theta}$  and  $90^\circ$ . Given  $\check{\theta}$ , we also have

$$\begin{aligned} \theta_{K, 2} &= \theta_{K, 1} - \check{\theta} \\ \theta_{1, 2} &= \theta_{1, 1} - \check{\theta}, \end{aligned} \quad (13)$$

where  $\sin \theta_1 < \sin \theta_2 < \dots < \sin \theta_K$ . From (12) and (13), we have

$$\cos(\theta_{K, 1}) - \cos(\theta_{1, 1}) = (\Delta s_{\theta, max, 1} - \frac{(\Delta s_{\theta, max, 2})}{\cos \check{\theta}}) / \tan \check{\theta} \quad (14)$$

Using trigonometric identities, from (12) and (14), the sum of the smallest and largest angles  $\theta_S = \theta_{1, 1} + \theta_{K, 1}$  is given by

$$\theta_S = 2 \arctan \frac{\frac{\Delta s_{\theta, max, 2}}{\cos \check{\theta}} - (\Delta s_{\theta, max, 1})}{(\Delta s_{\theta, max, 1} \tan \check{\theta})}. \quad (15)$$

The largest angle  $\theta_K$  is then derived from (12) and (15) as

$$\sin\left(\frac{2\theta_{K, 1} - \theta_S}{2}\right) = \frac{\Delta s_{\theta, max, 1}}{2 \cos(\theta_S/2)}. \quad (16)$$

By (15) and (16), we obtain

$$\begin{aligned} \theta_{K, 1} &= \text{asin}\left(\frac{\Delta s_{\theta, max, 1}}{2 \cos(\theta_S/2)}\right) + \frac{\theta_S}{2}, \\ \theta_{1, 1} &= \theta_S - \theta_{K, 1}. \end{aligned} \quad (17)$$

After obtaining  $\sin \theta_1$  and  $\sin \theta_K$ , the corresponding  $\Delta s_{\theta, max, 1}$  and  $\Delta s_{\theta, max, 2}$  are removed from the estimated

results and the second largest pair of signals  $\sin \theta_2$  and  $\sin \theta_{K-1}$  becomes the largest pair, which can be determined by re-applying (17). If the number of incident signals is even, all DOAs of remaining signals can be identified by repeating this procedure.

However, if there are odd number of incident signals, the  $(\frac{K+1}{2})$ -th signal is left after the above process and may still suffer from the mirroring ambiguity, which means  $\Delta s_{\theta, \tilde{k}, 1, 1}$  could represent either  $\sin \theta_{\tilde{k}, 1} - \sin \theta_{1, 1}$  or  $\sin \theta_{K, 1} - \sin \theta_{\tilde{k}, 1}$ .

As a result, with the different sinusoidal distance  $\Delta s_{\theta, \tilde{k}, 1, 1}$  between  $\theta_{1, 1}$  and  $\theta_{\tilde{k}, 1}$ , there are two possible solutions: the true DOA  $\theta_{\tilde{k}, 1}$  and its mirroring versions  $\bar{\theta}_{\tilde{k}, 1}$ :

$$\begin{aligned} \theta_{\tilde{k}, 1} &= \text{asin}(\Delta s_{\theta, \tilde{k}, 1, 1} + \sin(\theta_{1, 1})), \\ \bar{\theta}_{\tilde{k}, 1} &= \text{asin}(\sin(\theta_{K, 1}) - \Delta s_{\theta, \tilde{k}, 1, 1}). \end{aligned} \quad (18)$$

Similarly, there are also two possible solutions on the second array: true DOA  $\theta_{\tilde{k}, 2}$  and its mirroring version  $\bar{\theta}_{\tilde{k}, 2}$ . Defining  $\Theta_1 = [\theta_{\tilde{k}, 1}, \bar{\theta}_{\tilde{k}, 1}]$  and  $\Theta_2 = [\theta_{\tilde{k}, 2}, \bar{\theta}_{\tilde{k}, 2}]$  and with a known inter-array angle  $\check{\theta}$ , the DOA of the  $\tilde{k}$ -th DOA will be identified by the intersection of  $\Theta_2 - \check{\theta}$  and  $\Theta_1$  as  $\theta_{\tilde{k}, 1} = \Theta_1 \cap (\Theta_2 - \check{\theta})$ .

Thus, based on the dual-array structure, all DOAs can be identified with non-coherent measurements unambiguously without the need of reference signals.

## B. JOINT GROUP SPARSITY BASED METHOD

The above subsection indicates that, the magnitude-only measurements of the dual-array carry enough information to uniquely identify the DOAs of the impinging signals. Thus, instead of estimating two sets of sinusoidal differences  $\Delta s_{\theta, kk', 1}$  and  $\Delta s_{\theta, kk', 2}$  separately and then working out their true values, an effective joint group sparsity based method is proposed to find the DOAs directly.

The measurements at the dual-array can be expressed jointly as

$$\mathbf{Y} = |\mathbf{A}\mathbf{S}| + \mathbf{N}, \quad (19)$$

where  $\mathbf{Y} = [\mathbf{Y}_1^T, \mathbf{Y}_2^T]^T$ ,  $\mathbf{S} = [\mathbf{s}[1], \dots, \mathbf{s}[p]]$ ,  $\mathbf{N} = [\mathbf{N}_1^T, \mathbf{N}_2^T]^T$ , and  $\mathbf{A} = [\mathbf{A}_1^T, \mathbf{A}_2^T]$ . Since the first sensor is shared, when forming  $\mathbf{A}$  and  $\mathbf{Y}$ , we can choose to remove the corresponding rows of  $\mathbf{A}_2$  and  $\mathbf{Y}_2$ .

Consider the sparse steering matrix defined in (10), it is obvious that incident signals from an arbitrary arriving angle would share the same spatial support of  $\tilde{\mathbf{A}}_1$  and  $\tilde{\mathbf{A}}_2$ , although the DOAs with respect to each of them are different. As a result, for a sparse overcomplete representation, (19) can be expressed as

$$\mathbf{Y} = |\tilde{\mathbf{A}}\tilde{\mathbf{S}}| + \mathbf{N}, \quad (20)$$

where  $\tilde{\mathbf{S}} = [\tilde{\mathbf{s}}[1], \dots, \tilde{\mathbf{s}}[P]]$  and the measurement matrix  $\tilde{\mathbf{A}}$  is defined as

$$\tilde{\mathbf{A}} = [\tilde{\mathbf{A}}_1^T, \tilde{\mathbf{A}}_2^T]^T. \quad (21)$$

Finally, the joint group sparsity based non-coherent DOA estimation problem can be formulated as follows

$$\begin{aligned} \min \quad & \|\tilde{\mathbf{S}}\|_{2,0} \\ \text{s.t.} \quad & \|\mathbf{Y} - \tilde{\mathbf{A}}\tilde{\mathbf{S}}\|_F^2 < \varepsilon \end{aligned} \quad (22)$$

where  $\varepsilon$  is the upper bound of the reconstruction error.

Since the  $l_0$  norm is nonconvex, its relaxed version  $l_1$  norm is employed instead [18], and the resulting estimation problem can be solved by the following unconstrained optimisation problem

$$\min_{\tilde{\mathbf{S}}} \|\tilde{\mathbf{A}}\tilde{\mathbf{S}} - \mathbf{Y}\|_F^2 + \rho\|\tilde{\mathbf{S}}\|_{2,1}, \quad (23)$$

where  $\rho$  is the regularization parameter, and the  $\|\cdot\|_{2,1}$  is  $l_{2,1}$  norm, which promotes the row sparsity of  $\tilde{\mathbf{S}}$  by taking the  $l_2$  norm of its row vectors, forming a new column vector, and finally taking the  $l_1$  norm of the new column vector.

Clearly, the first term in objective function (23) is non-convex and results in the optimization problem NP-hard. However, this non-convex problem can be replaced by a surrogate convex function via the majorization-minimization (MM) method. Under the MM framework, a non-increasing property hold as [16], [19]

$$f(\mathbf{s}^{q+1}) \leq g(\mathbf{s}_{q+1}|\mathbf{s}^q) \leq g(\mathbf{s}^q|\mathbf{s}^q) = f(\mathbf{s}^q), \quad (24)$$

where  $f(\mathbf{s})$  is the original function,  $q$  indicates the iteration index and  $g(\mathbf{s}|\mathbf{s}_k)$  is the majorization function satisfying

$$\begin{aligned} g(\mathbf{s}|\mathbf{s}^q) &\geq f(\mathbf{s}), \quad \forall \mathbf{s}, \\ g(\mathbf{s}^q|\mathbf{s}^q) &= f(\mathbf{s}^q). \end{aligned} \quad (25)$$

By applying the PRIME technique [16], this non-convex problem can be majorized by a surrogate function. Considering the problem (23) with one snapshot and dropping the time index  $p$  for convenience, we have

$$\min_{\tilde{\mathbf{s}}} \|\tilde{\mathbf{A}}\tilde{\mathbf{s}} - \mathbf{y}\|_2^2 + \rho\|\tilde{\mathbf{s}}\|_1. \quad (26)$$

By following the same approach in [16], the above minimization problem (26) can be reformulated as

$$\begin{aligned} \min_{\tilde{\mathbf{s}}} \sum_{i=1}^N (|\tilde{\mathbf{a}}_i\tilde{\mathbf{s}}|^2 - 2y_i|\tilde{\mathbf{a}}_i\tilde{\mathbf{s}}| + |y_i|^2) + \rho\|\tilde{\mathbf{s}}\|_1 \\ = \min_{\tilde{\mathbf{s}}} \sum_{i=1}^N (|\tilde{\mathbf{a}}_i\tilde{\mathbf{s}}|^2 - 2y_i|\tilde{\mathbf{a}}_i\tilde{\mathbf{s}}|) + \rho\|\tilde{\mathbf{s}}\|_1, \end{aligned} \quad (27)$$

where  $\tilde{\mathbf{a}}_i$  represents the  $i$ -th row of the steering matrix  $\tilde{\mathbf{A}}$ , and  $y_i$  is the  $i$ -th component of  $\mathbf{y}$ . According to the Cauchy-Schwarz inequality, it has

$$\text{Re}(\tilde{\mathbf{a}}_i\tilde{\mathbf{s}}(\tilde{\mathbf{s}}^q)^H \tilde{\mathbf{a}}_i^H) \leq |\tilde{\mathbf{a}}_i\tilde{\mathbf{s}}||\tilde{\mathbf{a}}_i\tilde{\mathbf{s}}^q|, \quad (28)$$

where  $\text{Re}(\cdot)$  represents real part of its variable. Thus, (27) can be majorized as

$$\min_{\tilde{\mathbf{s}}} \sum_{i=1}^N (|\tilde{\mathbf{a}}_i\tilde{\mathbf{s}}|^2 - 2|y_i| \frac{\text{Re}(\tilde{\mathbf{a}}_i\tilde{\mathbf{s}}(\tilde{\mathbf{s}}^q)^H \tilde{\mathbf{A}}_i^H)}{|\tilde{\mathbf{a}}_i\tilde{\mathbf{s}}^q|}) + \rho\|\tilde{\mathbf{s}}\|_1, \quad (29)$$

which can be formulated as

$$\min_{\tilde{\mathbf{s}}} \|\tilde{\mathbf{A}}\tilde{\mathbf{s}} - \mathbf{c}^q\|_2^2, \quad \text{with} \quad \mathbf{c}^q = \mathbf{y} \odot e^{j\arg(\tilde{\mathbf{A}}\tilde{\mathbf{s}}^q)}, \quad (30)$$

where  $\odot$  denotes the Hadamard product,  $\tilde{\mathbf{s}}^q$  is a known complex vector and  $\arg(\cdot)$  represents the phase of its variable applied element-wise.

Thus, applying the same approach described in (30) column by column to the objective function, the original objective function (23) is majorized as

$$\min_{\tilde{\mathbf{S}}} \|\tilde{\mathbf{A}}\tilde{\mathbf{S}} - \mathbf{C}^q\|_F^2 + \rho\|\tilde{\mathbf{S}}\|_{2,1}, \quad (31)$$

where

$$\mathbf{C}^q = \mathbf{Y} \odot e^{j\arg(\tilde{\mathbf{A}}\tilde{\mathbf{S}}^q)}. \quad (32)$$

Since (31) is convex, it can be solved by the proximal gradient method [20], [21], which aims at solving problems in the form of

$$\min_{\tilde{\mathbf{S}}} F(\tilde{\mathbf{S}}) + G(\tilde{\mathbf{S}}), \quad (33)$$

where both  $F(\tilde{\mathbf{S}})$  and  $G(\tilde{\mathbf{S}})$  are convex and  $F(\tilde{\mathbf{S}})$  is differentiable. Then, this method iteratively refines its solution by

$$\tilde{\mathbf{S}}^{q+1} = \text{prox}_{\lambda G}(\tilde{\mathbf{S}}^q - \lambda \nabla F(\tilde{\mathbf{S}}^q)), \quad (34)$$

where  $\lambda$  is the stepsize and  $\nabla F(\tilde{\mathbf{S}}^q) = 2\tilde{\mathbf{A}}^H(\tilde{\mathbf{A}}\tilde{\mathbf{S}}^q - \mathbf{C})$  is the gradient of  $F(\tilde{\mathbf{S}})$ . The proximal operator  $\text{prox}$  is defined as

$$\text{prox}_{\lambda G}(\tilde{\mathbf{S}}) = \underset{\mathbf{Z}}{\text{argmin}} (\frac{1}{2\lambda}\|\mathbf{Z} - \tilde{\mathbf{S}}\|_F^2 + G(\mathbf{Z})). \quad (35)$$

Therefore, substituting the first term of object function (23) as  $F(\tilde{\mathbf{S}})$  and second term as  $G(\tilde{\mathbf{S}})$ ,  $\tilde{\mathbf{S}}^{q+1}$  can be obtained by solving the following problem

$$\tilde{\mathbf{S}}^{q+1} = \underset{\mathbf{Z}}{\text{argmin}} \{ \|\frac{1}{2\lambda}\mathbf{Z} - (\tilde{\mathbf{S}}^q - \lambda \nabla F(\tilde{\mathbf{S}}^q))\|_F^2 + \rho\|\mathbf{Z}\|_{2,1} \}. \quad (36)$$

Since  $G(\tilde{\mathbf{S}}) = \|\cdot\|_{2,1}$  is separable as  $\|\tilde{\mathbf{S}}\|_{2,1} = \sum_{i=1}^G \|\tilde{\mathbf{s}}_i\|_2$ , where  $\tilde{\mathbf{s}}_i$  represents the  $i$ -th row of  $\tilde{\mathbf{S}}$ , the proximal operator can be applied to each row independently as [22], [23]

$$\tilde{\mathbf{s}}_i^{q+1} = \underset{\mathbf{z}_i}{\text{argmin}} \{ \gamma\|\mathbf{z}_i\|_2 + \frac{1}{2\lambda}\|\mathbf{z}_i - (\tilde{\mathbf{s}}_i^q - \lambda \nabla F(\tilde{\mathbf{s}}_i^q))\|_2^2 \}, \quad (37)$$

where  $\mathbf{z}_i$  is the  $i$ -th row of  $\mathbf{Z}$ ,

$$\nabla F(\tilde{\mathbf{s}}_i^q) = 2(\tilde{\mathbf{A}}^H)_i(\tilde{\mathbf{A}}\tilde{\mathbf{s}}_i^q - \mathbf{C}^q), \quad i = 1, \dots, G, \quad (38)$$

is the  $i$ -th row of  $\nabla F(\tilde{\mathbf{S}}^q)$ , and  $(\tilde{\mathbf{A}}^H)_i$  is the  $i$ -th row of  $\tilde{\mathbf{A}}^H$ . This is equivalent to applying the row-wise proximal operator of  $l_2$  norm to (36), which has an analytical solution as [23]

$$\tilde{\mathbf{s}}_i^{q+1} = (\tilde{\mathbf{s}}_i^q - \lambda \nabla F(\tilde{\mathbf{s}}_i^q)) \max(1 - \frac{\rho\lambda}{\|\tilde{\mathbf{s}}_i^q - \lambda \nabla F(\tilde{\mathbf{s}}_i^q)\|_2}, 0). \quad (39)$$

The positions of non-zero rows of the reconstructed signal matrix  $\tilde{\mathbf{S}}^q$  correspond to DOAs of incident signals.

### C. CONVERGENCE ANALYSIS

The non-convex group sparse phase retrieval problem is replaced by a convex surrogate via the majorization-minimization technique. If the second inequality of (24) holds, we have

$$\begin{aligned} \|\tilde{\mathbf{A}}\tilde{\mathbf{S}}^{q+1} - \mathbf{C}^q\|_F^2 + \rho\|\tilde{\mathbf{S}}^{q+1}\|_{2,1} \\ \leq \|\tilde{\mathbf{A}}\tilde{\mathbf{S}}^q - \mathbf{C}^q\|_F^2 + \rho\|\tilde{\mathbf{S}}^q\|_{2,1}, \end{aligned} \quad (40)$$

and thus the generated sequence  $\tilde{\mathbf{S}}^q$  will at least converge to a stationary point.

Following the convergence analysis of the proximal gradient method in [24], [25], next we give an analysis of the derived algorithm.

Consider the general model (31),  $F(\mathbf{S}) = \|\tilde{\mathbf{A}}\tilde{\mathbf{S}} - \mathbf{C}^q\|_F^2$  and  $G(\tilde{\mathbf{S}}) = \rho\|\tilde{\mathbf{S}}\|_{2,1}$ . The smallest Lipschitz constant of  $F(\mathbf{S})$  is the Hessian of it, which is equal to  $L = 2\lambda_{\max}(\tilde{\mathbf{A}}^H\tilde{\mathbf{A}})$ . Thus, if  $\lambda \leq \frac{1}{L}$ , for any  $\tilde{\mathbf{S}}^q$ ,  $F(\tilde{\mathbf{S}}^{q+1})$  is upper bounded by [24],

$$F(\tilde{\mathbf{S}}^{q+1}) \leq F(\tilde{\mathbf{S}}^q) + \text{Re}(\langle \nabla F(\tilde{\mathbf{S}}^q), \tilde{\mathbf{S}}^{q+1} - \tilde{\mathbf{S}}^q \rangle) + \frac{1}{2\lambda} \|\tilde{\mathbf{S}}^{q+1} - \tilde{\mathbf{S}}^q\|_F^2, \quad (41)$$

where  $\langle \cdot, \cdot \rangle$  represents Frobenius inner product and  $\text{Re}(\cdot)$  represents real part of its variable. Since the  $l_{2,1}$  norm is also convex, for  $\tilde{\mathbf{S}}^q$ , there should be a subgradient  $\mathbf{V} \in \partial\|\tilde{\mathbf{S}}^{q+1}\|_{2,1}$ , which satisfies

$$G(\tilde{\mathbf{S}}^{q+1}) \leq G(\tilde{\mathbf{S}}) - \text{Re}(\langle \mathbf{V}, \tilde{\mathbf{S}} - \tilde{\mathbf{S}}^{q+1} \rangle). \quad (42)$$

Therefore, using (41) and (42), the upper bound of the objective function (31) is given by

$$F(\tilde{\mathbf{S}}^{q+1}) + G(\tilde{\mathbf{S}}^{q+1}) \leq F(\tilde{\mathbf{S}}^q) + G(\tilde{\mathbf{S}}^q) - \text{Re}(\langle \mathbf{V}, \tilde{\mathbf{S}}^q - \tilde{\mathbf{S}}^{q+1} \rangle) + \text{Re}(\langle \nabla F(\tilde{\mathbf{S}}^q), \tilde{\mathbf{S}}^q - \tilde{\mathbf{S}}^{q+1} \rangle) + \frac{1}{2\lambda} \|\tilde{\mathbf{S}}^{q+1} - \tilde{\mathbf{S}}^q\|_F^2. \quad (43)$$

The sequence  $\tilde{\mathbf{S}}^q$  is generated by the proximal gradient method, which can be written as

$$\begin{aligned} \tilde{\mathbf{S}}^{q+1} &= \text{prox}_{\lambda g}(\tilde{\mathbf{S}}^q - \lambda \nabla F(\tilde{\mathbf{S}}^q)) \\ &= \underset{\mathbf{Z}}{\text{argmin}}(G(\mathbf{Z}) + \frac{1}{2\lambda} \|\mathbf{Z} - (\tilde{\mathbf{S}}^q - \lambda \nabla F(\tilde{\mathbf{S}}^q))\|_F^2) \\ &= \underset{\mathbf{Z}}{\text{argmin}}(G(\mathbf{Z}) + F(\tilde{\mathbf{S}}^q) + \langle \nabla F(\tilde{\mathbf{S}}^q), \mathbf{Z} - \tilde{\mathbf{S}}^q \rangle + \frac{1}{2\lambda} \|\mathbf{Z} - \tilde{\mathbf{S}}^q\|_F^2). \end{aligned} \quad (44)$$

The last equality is obtained by ignoring constant terms unrelated to  $\mathbf{Z}$ .

With the optimal condition of (44), if  $\tilde{\mathbf{S}}^{q+1}$  exists, its subgradient  $\mathbf{V} \in \partial\|\tilde{\mathbf{S}}^{q+1}\|_{2,1}$  should satisfy

$$\mathbf{V} + \frac{1}{\lambda}(\tilde{\mathbf{S}}^{q+1} - \tilde{\mathbf{S}}^q) + \nabla F(\tilde{\mathbf{S}}^q) = \mathbf{0}. \quad (45)$$

Thus, by substituting (45) into (43), one has

$$F(\tilde{\mathbf{S}}^q) + G(\tilde{\mathbf{S}}^q) - F(\tilde{\mathbf{S}}^{q+1}) - G(\tilde{\mathbf{S}}^{q+1}) \geq \frac{1}{2\lambda} \|\tilde{\mathbf{S}}^q - \tilde{\mathbf{S}}^{q+1}\|_F^2. \quad (46)$$

Therefore, the sequence  $\tilde{\mathbf{S}}^q$  produced by the proximal gradient method is guaranteed to converge with stepsize  $\lambda \leq \frac{1}{L}$ .

## D. ACCELERATION SCHEME

Since the group sparse phase retrieval problem is transformed into a convex surrogate and solved by the proximal gradient method, it can be further accelerated by applying the Nesterov acceleration [25], [26].

## Algorithm 1 Summary (ToyBar)

**Input:**  $\tilde{\mathbf{A}}, \mathbf{Y}, \gamma, \lambda,$

**Output:**  $\tilde{\mathbf{S}}$  (reconstructed signal).

**Initialization:** Set  $\tilde{\mathbf{S}}^0$  as a random matrix,  $\mathbf{B}^0 = \tilde{\mathbf{S}}^0$ ,  $\beta^0 = 1$ .

**General steps:** for  $q = 0, \dots, Q$

1) Calculate  $\mathbf{C}^q = \mathbf{Y} \odot e^{j\text{arg}(\tilde{\mathbf{A}}\mathbf{B}^q)}$

2) Calculate  $\tilde{\mathbf{S}}^{q+1}$ , for  $i = 1, \dots, G$

**Gradient:**  $\nabla F(\mathbf{b}_i^q) = 2(\tilde{\mathbf{a}}^q)_i(\tilde{\mathbf{A}}\mathbf{B}^q - \mathbf{C}^q)$ ,

Find  $\tilde{\mathbf{s}}_i^{q+1}$  as  $\tilde{\mathbf{s}}_i^{q+1} = (\mathbf{b}_i^q - \lambda \nabla F(\mathbf{b}_i^q))$

$\max(1 - \frac{\rho\lambda}{\|\mathbf{b}_i^q - \lambda \nabla F(\mathbf{b}_i^q)\|_2}, 0)$ ,

where  $\mathbf{b}_i^q$  is the  $i$ -th row of  $\mathbf{B}^q$ .

3) **Update:**  $\beta^{q+1} = \frac{1 + \sqrt{1 + 4(\beta^q)^2}}{2}$ ,

$\mathbf{B}^{q+1} = \tilde{\mathbf{S}}^{q+1} + \frac{\beta^q - 1}{\beta^{q+1}}(\tilde{\mathbf{S}}^{q+1}) - \tilde{\mathbf{S}}^q$ .

4)  $q = q + 1$ , go to 1).

This method does not apply proximal operator to previous  $\tilde{\mathbf{S}}^{q+1}$  directly, but another point  $\mathbf{B}^{q+1}$  based on  $\tilde{\mathbf{S}}^{q+1}$  and  $\tilde{\mathbf{S}}^q$  expressed as

$$\mathbf{B}^{q+1} = \tilde{\mathbf{S}}^{q+1} + \frac{\beta^q - 1}{\beta^{q+1}}(\tilde{\mathbf{S}}^{q+1} - \tilde{\mathbf{S}}^q), \quad (47)$$

where

$$\beta^{q+1} = \frac{1 + \sqrt{1 + 4(\beta^q)^2}}{2}. \quad (48)$$

The full algorithm is presented in the above Algorithm Summary, which is referred to as fasT grOup sparsitY Based phAsE Retrieval (ToyBar).

Note that, the proposed method does not work if there is only one incident signal due to lack of sinusoidal difference information  $\Delta s_{\theta, kk'}$ . Therefore, for such a scenario, an additional signal has to be deployed as a reference. However, different from existing methods, DOA of the additional signal does not need to be known in advance and its DOA will be estimated simultaneously together with other impinging signals.

## E. MAXIMUM NUMBER OF RESOLVABLE SIGNALS

Since the idea of the proposed non-coherent DOA estimation utilizes sinusoidal difference of two sub-arrays, the maximum number of signals that can be distinguished depends on the least number of sinusoidal differences that can be distinguished by the two individual sub-arrays. Since there are  $N$  and  $M$  subarray sensors, respectively, traditionally they can recovery  $N - 1$  and  $M - 1$  signals, and thus the dual array is able to reconstruct  $\min\{N - 1, M - 1\}$  signals.

However, due to the lack of phase information, from the viewpoint of phase retrieval, less than  $N - 1$  signals can be constructed with  $N$  measurements. In [27], it proves that for full sparse signals ( $K = G$ ), at most  $G = 2N - 1$  signals can be recovered with generic measurement frame  $\mathbf{A} = \{\mathbf{A}_n\}_{n=1}^N$  if both the measurement matrix and signals are real-valued,

where  $\mathbf{A}_n$  is the  $n$ -th row of  $\mathbf{A}$  and by generic it means  $\mathbf{A}$  is an open dense subset of  $\mathbb{R}(\mathbb{C})$  i.e. random Gaussian matrix. For the complex-valued scenario, [28] conjectures that  $N = 4G - 4$  generic measurements is required to recover  $G$  signals. This conjecture has been proved in [29] for  $G = 2^b - 1$ ,  $b \geq 1$ . For  $K$ -sparse signals,  $4K - 1$  ( $8K - 2$ ) generic measurements are needed for real (complex) scenarios [30].

Since the steering matrix is not generic, the above condition might not hold for the non-coherent measurements of an array. The authors in [31] show that  $K^2 - K + 1$  measurements are required to recover  $K$  signals with Fourier magnitude measurements by pointing out that reconstructing  $K$ -sparse signals from its magnitude measurements is the same as recovering its auto-correlation from its Fourier measurements. As the steering matrix has a similar structure to the Fourier measurements matrix, similar theorem can be derived by the same approach proposed in [31].

*Theorem 1:* To reconstruct a  $K$ -sparse signals  $\mathbf{s}$ , at least  $K^2 - K + 1$  measurements are necessary.

*Proof:* Defining a vector  $\mathbf{u}$  as

$$\mathbf{u} = [|\mathbf{s}|^2, \mathbf{s}_{1,K}, \dots, \mathbf{s}_{K-1,K}, \mathbf{s}_{K-1,K}^*, \dots, \mathbf{s}_{1,K}^*]^T, \quad (49)$$

where  $\mathbf{s}_{k,K} = [s_k s_{k+1}^*, s_k s_{k+2}^*, \dots, s_k s_K^*]$  for  $k = 1, \dots, K - 1$ , and  $|\mathbf{s}|^2 = \sum_{k=1}^K |s_k|^2$ .

Then, we can find a matrix  $\mathbf{D}$  satisfying

$$|\tilde{\mathbf{A}}\tilde{\mathbf{s}}|^2 = \mathbf{D}\mathbf{u}, \quad (50)$$

□

with

$$\mathbf{d}_n^T = \begin{bmatrix} 1 \\ e^{-jn\alpha \Delta \sin \theta_{1,K}} \\ \vdots \\ e^{-jn\alpha \Delta \sin \theta_{K-1,K}} \\ e^{jn\alpha \Delta \sin \theta_{K-1,K}} \\ \vdots \\ e^{jn\alpha \Delta \sin \theta_{1,K}} \end{bmatrix}, \quad (51)$$

where  $\Delta \sin \theta_{k,K} = [\sin \theta_k - \sin \theta_{k+1}, \dots, \sin \theta_k - \sin \theta_K]$ . Therefore, recovering  $\tilde{\mathbf{s}}$  from its magnitude measurements is equivalent to reconstructing  $\mathbf{u}$  with measurement matrix  $\mathbf{D}$ . For an  $N$ -element array, it can recover up to  $K$  signals, with  $K$  satisfying  $K^2 - K + 1 \leq N$ . Note that, this is not a tight bound and only used as a reference.

### F. CRAMÉR-RAO BOUND

In this section, the CRB for non-coherent DOA estimation is derived. Although an approximation expression of CRB for non-coherent DOA estimation was derived in [11], [12], a high gain reference signal has to be applied at one end of interested range, which is not applicable to the signal model in this paper. Since the reconstructed signals are up to a global phase factor, for complex signal  $\mathbf{s}$ , the Fisher information matrix (FIM) would be singular [32], [33]. Thus, in this work, instead of estimating the phase information of signals, only phase differences between signals are considered.

From (19), the probability density function is expressed as

$$p(\mathbf{Y}; \Phi) = \prod_p \prod_{n=0}^{M+N-1} \frac{1}{2\pi\sigma_n^2} e^{(y_n[p] - |\mathbf{a}_n \mathbf{s}[p]|)^2 / 2\sigma_n^2}, \quad (52)$$

where  $\mathbf{a}_n$  and  $\mathbf{y}_n$  represent the  $n$ -th row of  $\mathbf{A}$  and  $\mathbf{Y}$ , separately. From the signal model the unknown parameter vector of arriving angles, magnitude, phase difference and noise level can be represented as

$$\begin{aligned} \Phi &= [\boldsymbol{\theta}, |\mathbf{s}|, \Delta\boldsymbol{\gamma}, \sigma^2]^T \\ \boldsymbol{\theta} &= [\theta_1, \dots, \theta_K], \\ |\mathbf{s}[p]| &= [ |s_1[p]|, \dots, |s_K[p]| ], \\ \Delta\boldsymbol{\gamma} &= [\Delta\gamma_{12}, \Delta\gamma_{13}, \dots, \Delta\gamma_{(K-1)K}], \end{aligned} \quad (53)$$

where  $\Delta\gamma_{kk'} = \gamma_k - \gamma_{k'}$ ,  $\gamma_k$  is the phase of the  $k$ -th signals and  $\sigma^2$  is noise power. Since there are  $\frac{K^2-K}{2}$  cross terms in  $|\tilde{\mathbf{A}}\tilde{\mathbf{s}}|$ , there are also  $\frac{K^2-K}{2}$  entries in  $\Delta\boldsymbol{\gamma}$ . For deterministic but unknown  $\mathbf{AS}$ , the FIM is defined as

$$\mathbf{FIM}(\Phi) = \mathbb{E} \left\{ \frac{\partial \ln^2 p(\mathbf{Y}; \Phi)}{\partial \Phi \partial \Phi^T} \right\} \quad (54)$$

The  $\{i, j\}$ -th entry of the FIM  $\mathbf{F}$  is given by [34]

$$\begin{aligned} \mathbf{F}_{i,j} &= \left[ \frac{\partial \boldsymbol{\mu}(\Phi)}{\partial \Phi_i} \right]^T \boldsymbol{\Gamma}^{-1}(\Phi) \left[ \frac{\partial \boldsymbol{\mu}(\Phi)}{\partial \Phi_j} \right] \\ &+ \frac{1}{2} \left[ \boldsymbol{\Gamma}^{-1}(\Phi) \frac{\partial \boldsymbol{\Gamma}^{-1}(\Phi)}{\partial \Phi_i} \boldsymbol{\Gamma}^{-1}(\Phi) \frac{\partial \boldsymbol{\Gamma}^{-1}(\Phi)}{\partial \Phi_j} \right], \end{aligned} \quad (55)$$

where  $\boldsymbol{\Gamma}^{-1}(\Phi) = \frac{1}{\sigma_n^2} \mathbf{I}_{M+N-1}$  and  $\mathbf{I}_{M+N-1}$  is the identity matrix and  $\boldsymbol{\mu}(\Phi) = |\mathbf{AS}|$ . Since  $\boldsymbol{\mu}(\Phi)$  is independent with the noise level, we have

$$\mathbf{F} = \begin{bmatrix} \tilde{\mathbf{F}} & \mathbf{0} \\ \mathbf{0} & \mathbf{F}_\sigma \end{bmatrix} + \begin{bmatrix} \mathbf{0} & \mathbf{0} \\ \mathbf{0} & \mathbf{F}_\sigma \end{bmatrix}, \quad (56)$$

where the DOA related block is in  $\tilde{\mathbf{F}}$  and its  $\{i, j\}$ -th entry is expressed as

$$\tilde{\mathbf{F}}_{i,j} = \left[ \frac{\partial \boldsymbol{\mu}(\Phi)}{\partial \Phi_i} \right]^T \boldsymbol{\Gamma}^{-1}(\Phi) \left[ \frac{\partial \boldsymbol{\mu}(\Phi)}{\partial \Phi_j} \right], \quad (57)$$

where  $(\cdot)^{-1}$  is the matrix inverse operator. As the FIM is block diagonal,  $\mathbf{F}_\sigma$  has no effect on CRB result of DOAs. Thus, CRB of DOAs can be determined by the inverse of  $\tilde{\mathbf{F}}$ .

Denotes  $|\mathbf{a}_n \mathbf{s}| = (\mathbf{s}^H \mathbf{a}_n^H \mathbf{a}_n \mathbf{s})^{\frac{1}{2}} = (\mathbf{s}^H \mathbf{A}_n \mathbf{s})^{\frac{1}{2}}$  and drop index  $p$  for convenience, we have

$$\begin{aligned} \frac{\partial |\mathbf{a}_n \mathbf{s}|}{\partial \theta_k} &= \frac{1}{2} (\mathbf{s}^H \mathbf{A}_n \mathbf{s})^{\frac{1}{2}} \frac{\partial (\mathbf{s}^H \mathbf{A}_n \mathbf{s})}{\partial \theta_k} \\ &= \frac{1}{2} (\mathbf{s}^H \mathbf{A}_n \mathbf{s})^{-\frac{1}{2}} \left( jn\alpha \cos \theta_k s_k^* \mathbf{A}_n(k, :) \right. \\ &\quad \left. - jn\alpha \cos \theta_k s_k \mathbf{s}^H \mathbf{A}_n(:, k) \right) \\ &= (\mathbf{s}^H \mathbf{A}_n \mathbf{s})^{-\frac{1}{2}} \text{Im} \left( -n\alpha \cos \theta_k s_k^* \mathbf{A}_n(k, :) \mathbf{s} \right) \\ \frac{\partial |\mathbf{a}_n \mathbf{s}|}{\partial |s|_k} &= \frac{1}{2} (\mathbf{s}^H \mathbf{A}_n \mathbf{s})^{-\frac{1}{2}} \frac{\partial (\mathbf{s}^H \mathbf{A}_n \mathbf{s})}{\partial |s|_k} \\ &= \frac{1}{2} (\mathbf{s}^H \mathbf{A}_n \mathbf{s})^{-\frac{1}{2}} (e^{-j\gamma_k} \mathbf{A}_n(k, :) \mathbf{s} \\ &\quad + e^{j\gamma_k} \mathbf{s}^H \mathbf{A}_n(:, k)) \\ &= (\mathbf{s}^H \mathbf{A}_n \mathbf{s})^{-\frac{1}{2}} \text{Re} \left( e^{j\gamma_k} \mathbf{s}^H \mathbf{A}_n(:, k) \right) \end{aligned}$$

$$\begin{aligned} \frac{\partial |\mathbf{a}_n \mathbf{s}|}{\partial \Delta \gamma_{kk'}} &= \frac{1}{2} (\mathbf{s}^H \mathbf{A}_n \mathbf{s})^{-\frac{1}{2}} \frac{\partial (\mathbf{s}^H \mathbf{A}_n \mathbf{s})}{\partial \Delta \gamma_{kk'}} \\ &= \frac{1}{2} (\mathbf{s}^H \mathbf{A}_n \mathbf{s})^{-\frac{1}{2}} (-j s_k^* \mathbf{A}_n(k, k') s_{k'} \\ &\quad + j s_k s_{k'}^* \mathbf{A}_n(k', k)) \\ &= (\mathbf{s}^H \mathbf{A}_n \mathbf{s})^{-\frac{1}{2}} \text{Im}(s_k s_{k'}^* \mathbf{A}_n(k', k)), \end{aligned} \quad (58)$$

where  $(\cdot)^*$  is the complex conjugate operator,  $\mathbf{A}_n(k, \cdot)$  is the  $k$ -th row of  $\mathbf{A}_n$  and  $\mathbf{A}_n(\cdot, k)$  is the  $k$ -th column of  $\mathbf{A}_n$ . Substituting (58) into (56), the FIM can be obtained as

$$\tilde{\mathbf{F}} = \sum_{p=1}^P \frac{1}{\sigma_n^2} \mathbf{G}[p] \mathbf{G}[p]^H, \quad (59)$$

where

$$\mathbf{G}[p] = \begin{bmatrix} \text{Im}(\text{diag}(\mathbf{s}[p]^*) (\mathbf{E} \odot \mathbf{A})^H \text{diag}(\mathbf{A} \mathbf{s}[p])) \tilde{\mathbf{y}}[p] \\ \text{Re}(\text{diag}(e^{-j\gamma} \mathbf{A}^H \text{diag}(\mathbf{A} \mathbf{s}[p])) \tilde{\mathbf{y}}[p] \\ -\text{Im}(\text{diag}\{\dot{\mathbf{s}}[p]\} \dot{\mathbf{A}} \odot \text{diag}\{\ddot{\mathbf{s}}[p]\} \ddot{\mathbf{A}}) \tilde{\mathbf{y}}[p] \end{bmatrix}, \quad (60)$$

with

$$\begin{aligned} \mathbf{E} &= [\mathbf{e}_1, \dots, \mathbf{e}_K], \\ \mathbf{e}_k &= [0, \alpha \cos \theta_{k,1}, \dots, (N-1)\alpha \cos \theta_{k,1}, \\ &\quad \alpha \cos \theta_{k,2}, \dots, (N-1)\alpha \cos \theta_{k,2}]^T, \\ \tilde{\mathbf{y}}[p] &= \text{diag}\{|\mathbf{A} \mathbf{s}[p]|^{-\frac{1}{2}}\}, \\ \dot{\mathbf{s}} &= [\underbrace{s_1[p], \dots, s_1[p]}_{K-1}, \underbrace{s_2[p], \dots, s_2[p]}_{K-2}, \dots, s_{K-1}[p]], \\ \dot{\mathbf{A}} &= [\mathbf{A}(:, 1)^T, \dots, \mathbf{A}(:, 1)^T, \dots, \mathbf{A}(:, K-1)^T], \\ \ddot{\mathbf{s}} &= [s_2^*[p], s_3^*[p], \dots, s_K^*[p], s_3^*[p], \dots, s_K^*[p], \dots, s_K^*[p]], \\ \ddot{\mathbf{A}} &= [\mathbf{A}(:, 2)^H, \dots, \mathbf{A}(:, K)^H, \dots, \mathbf{A}(:, K)^H]. \end{aligned} \quad (61)$$

The CRB associated with the DOA of signals can be obtained by the diagonal elements of the inverse FIM  $\tilde{\mathbf{F}}$ .

### G. GRID REFINEMENT

Similar to other compressive sensing based DOA estimation methods, the estimation results of the proposed method are dependent on the grid size in the angle domain. A denser grid usually leads to a more accurate DOA results, but with a much higher computational complexity [4].

Therefore, instead of creating a dense grid initially, a coarse grid is firstly made; based on the DOA results, a denser steering matrix is then built around the estimated locations of incident signals, and the algorithm is employed again to find a more accurate DOA.

### IV. SIMULATION RESULTS

In this section, performance of the proposed ToyBar is studied and compared with the modified GESPAR [7] for non-coherent DOA estimation. For the modified GESPAR, 64000 iterations are used. For the proposed algorithm, the iterations are fixed at  $Q = 400$  and 50 random initializations are used in order to find the global minimum of the

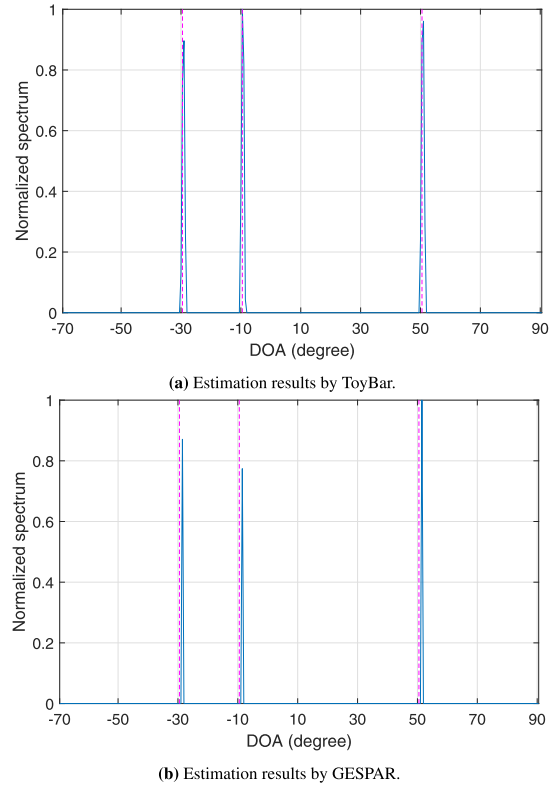


FIGURE 2. Estimation results based on the dual-array structure.

non-convex problem. Step size  $\lambda$  is set as  $1/(2\lambda_{\max}(\tilde{\mathbf{A}}^H \tilde{\mathbf{A}}))$ . The angle between the two subarrays is set as  $\theta = 20^\circ$  unless specified otherwise. Accordingly, the area of interest for the first array is set to  $[-70^\circ, 90^\circ]$  while for the second array it is  $[-90^\circ, 70^\circ]$ , with a step size of  $0.5^\circ$  for initial DOA estimation. After obtaining the initial DOA estimates  $\hat{\theta}_k$ , a new grid with step size  $0.05^\circ$  is formed around an interval of  $\hat{\theta}_k$ , which includes  $1.5^\circ$  to either side of it. i.e.  $0.05^\circ$  spacing within  $[\hat{\theta}_k - 1.5^\circ, \hat{\theta}_k + 1.5^\circ]$ . While applied the refine step to GESPAR, the iterations halved as the number of grids decreased. Results obtained with this refinement step are referred to as ‘‘ToyBar-Refined’’ and ‘‘GESPAR-Refined’’ in the following.

For the first set of measurements, the signal to noise ratio (SNR) is 15 dB and there are  $K = 3$  signals impinging on the array, with incident angles  $-30^\circ, -10^\circ$ , and  $50^\circ$  (relative to the first array). The number of snapshots is 20 and the number of sensors is  $M = N = 20$ . The spatial spectrum of estimation results is shown in Fig. 2, where Fig. 2(a) provides the result of ToyBar, while Fig. 2(b) is for GESPAR. The dotted lines represent the true incident angles. It can be seen that all 3 signals have been identified by both GESPAR and the proposed method. However, although GESPAR provides a sharper peak, it requires prior knowledge of the number of incident signals, while the proposed method does not.

Next, performances of the proposed ToyBar and GESPAR are evaluated with different SNR values ranging from 5 dB to 25 dB with three signals identical to the first experiment in terms of the root mean square error (RMSE), and the results

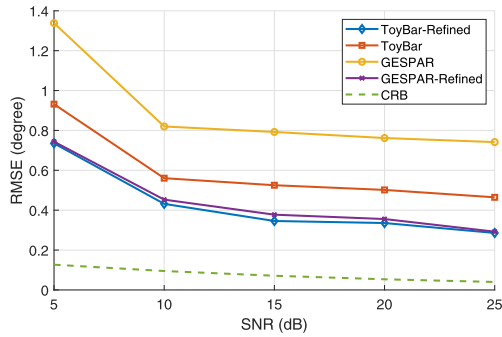


FIGURE 3. RMSEs versus different SNR.

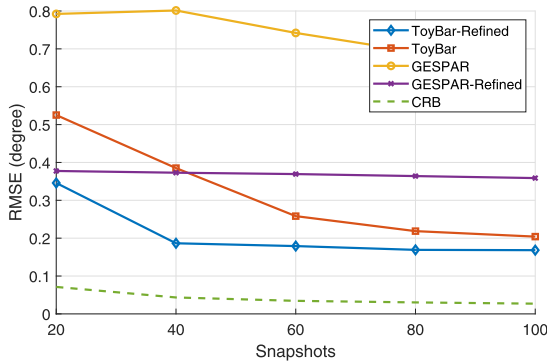


FIGURE 4. RMSEs versus number of snapshots.

are shown in Fig. 3, with each point obtained by averaging over 100 trials. Clearly, both algorithms have achieved more accurate results with increasing SNR, but the estimation of the proposed ToyBar is slightly more accurate than GESPAR; besides, the refined step is able to further improve the performance of both algorithms, but the refined ToyBar also outperforms the refined GESPAR.

In Fig. 4, results of RMSE versus the number of snapshots of both algorithms are provided. SNR is fixed at 15 dB but the number of snapshots  $P$  is from 20 to 100. Each point is averaged over 100 trials. Under all snapshot settings, the proposed algorithm has a lower RMSE than the modified GESPAR. In addition, compared to the proposed ToyBar, the modified GESPAR is less sensitive to snapshots.

To compare the computational complexity of GESPAR and the proposed ToyBar, the average computation time of both algorithms with different number of snapshots is listed in Table. 1, where the average running time of both algorithms are under CPU I5 5200U at 2.2GHz and 4 GB RAM. It can be seen that an increasing number of snapshots significantly increases the running time of GESPAR and it always requires much longer running time than the proposed method. This is because GESPAR is a greedy algorithm and requires more iterations to achieve a good performance; moreover, this algorithm was designed for traditional phase retrieval applications, which always assume the input signal has one snapshot and thus its modified version for multiple snapshots has to use multiple time samples separately. By contrast, the proposed algorithms exploits the multiple time samples jointly and requires less computation time than GESPAR. Similarly,

TABLE 1. Running times versus number of snapshots.

Snapshots	20	60	100
Toybar(s)	57.7	84.6	115.2
ToyBar-Refined(s)	89.2	134.1	181.4
GESPAR(s)	2154.2	6551.4	10816.5
GESPAR-Refined(s)	3384.7	10317.6	17045.5

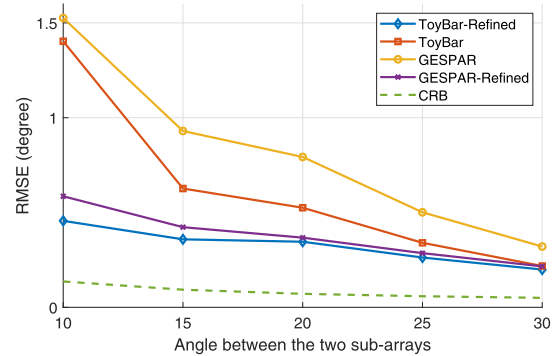


FIGURE 5. RMSE results versus  $\theta$  for SNR = 15 dB.

the computational complexity of GESPAR-Refined is also much higher than ToyBar-Refined.

Finally, the performance of the DOA estimation results under various angles  $\theta$  between the two arrays is examined. The RMSE results versus  $\theta$  is shown in Fig. 5. SNR= 15 dB and other simulation parameters are the same as the first simulation. It can be seen that, although a larger  $\theta$  always improves the estimation accuracy, the proposed Toybar has a better performance than the modified GESPAR. In addition, the refinement step can improve the performance of the proposed ToyBar and the modified GESPAR significantly when  $\theta$  is small. However, since the effective range of estimation is restricted by  $\theta$ ,  $\theta$  should be chosen carefully in order to cover more area within  $[-90^\circ, 90^\circ]$ .

V. CONCLUSION

The non-coherent DOA estimation problem with a dual-array structure has been studied and an efficient sparse phase retrieval algorithm called ToyBar for multiple snapshots is proposed. By exploiting the spatial information of both sub-arrays of the dual-array simultaneously, a joint group sparsity based non-coherent DOA estimation problem with multiple snapshots was formulated. This problem can be solved by the proximal gradient method after transforming the original non-convex problem to its convex surrogate via the majorization-minimization. With the proposed array structure, ambiguities associated with the magnitude-only measurements are avoided without the need of reference signals. Compared to the modified GESPAR, knowledge of number of incident signals is not required for the proposed algorithm. In addition, as demonstrated by simulations, ToyBar has a better performance in terms of both computational complexity and accuracy. One note is, recent study has shown that other array structures such as circular arrays can also be

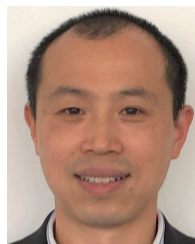
employed to overcome the underlying ambiguities instead of the proposed dual-array structure.

## REFERENCES

- [1] H. L. V. Tress, *Optimum Array Processing: Part IV of Detection, Estimation, and Modulation Theory*. New York, NY, USA: Wiley, 2002.
- [2] R. Schmidt, "Multiple emitter location and signal parameter estimation," *IEEE Trans. Antennas Propag.*, vol. 34, no. 3, pp. 276–280, Mar. 1986.
- [3] R. Roy and T. Kailath, "ESPRIT, Estimation of signal parameters via rotation invariance techniques," *IEEE Trans. Acoust., Speech, Signal Process.*, vol. 37, no. 7, pp. 984–995, Jul. 1989.
- [4] D. Malioutov, M. Cetin, and A. S. Willsky, "A sparse signal reconstruction perspective for source localization with sensor arrays," *IEEE Trans. Signal Process.*, vol. 53, no. 8, pp. 3010–3022, Aug. 2005.
- [5] Q. Shen, W. Liu, W. Cui, and S. Wu, "Underdetermined DOA estimation under the compressive sensing framework: A review," *IEEE Access*, vol. 4, pp. 8865–8878, Nov. 2016.
- [6] Q. Shen, W. Liu, W. Cui, S. Wu, Y. D. Zhang, and M. G. Amin, "Low complexity direction-of-arrival estimation based on wideband co-prime arrays," *IEEE Trans. Signal Process.*, vol. 64, no. 19, pp. 1445–1456, Oct. 2016.
- [7] H. Kim, A. M. Haimovich, and Y. C. Eldar, "Non-coherent direction of arrival estimation from magnitude-only measurements," *IEEE Signal Process. Lett.*, vol. 22, no. 7, pp. 925–929, Jul. 2015.
- [8] Y. Shechtman, A. Beck, and Y. C. Eldar, "GESPAR: Efficient phase retrieval of sparse signals," *IEEE Trans. Signal Process.*, vol. 62, no. 4, pp. 928–938, Feb. 2014.
- [9] C. R. Karanam, B. Korany, and Y. Mostofi, "Magnitude-based angle-of-arrival estimation, localization, and target tracking," in *Proc. 17th ACM/IEEE Int. Conf. Inf. Process. Sensor Netw. (IPSN)*, Apr. 2018, pp. 254–265.
- [10] M. Chowdhury, M. Rao, and A. Goldsmith, "Direction finding using non-coherent measurements in large antenna arrays," in *Proc. 51st Asilomar Conf. Signals, Syst., Comput.*, Oct. 2017, pp. 1231–1236.
- [11] W. Jiang and A. M. Haimovich, "Cramer-rao bound for noncoherent direction of arrival estimation in the presence of sensor location errors," *IEEE Signal Process. Lett.*, vol. 24, no. 9, pp. 1303–1307, Sep. 2017.
- [12] W. Jiang and A. M. Haimovich, "Cramer-rao bound and approximate maximum likelihood estimation for non-coherent direction of arrival problem," in *Proc. Annu. Conf. Inf. Syst. (CISS)*, Mar. 2016, pp. 506–510.
- [13] W. Wang, R. Wu, J. Liang, and H. C. So, "Phase retrieval approach for DOA estimation with array errors," *IEEE Trans. Aerosp. Electron. Syst.*, vol. 53, no. 5, pp. 2610–2620, Oct. 2017.
- [14] A. Liu, G. Liao, C. Zeng, Z. Yang, and Q. Xu, "An eigenstructure method for estimating DOA and sensor gain-phase errors," *IEEE Trans. Signal Process.*, vol. 59, no. 12, pp. 5944–5956, Dec. 2011.
- [15] Z. Wan and W. Liu, "Non-coherent DOA estimation based on a dual-array structure without reference signals," in *Proc. IEEE 8th Int. Workshop Comput. Adv. Multi-Sensor Adapt. Process. (CAMSAP)*, Dec. 2019, pp. 46–50.
- [16] T. Qiu, P. Babu, and D. P. Palomar, "PRIME: Phase retrieval via majorization-minimization," *IEEE Trans. Signal Process.*, vol. 64, no. 19, pp. 5174–5186, Oct. 2016.
- [17] Y. Shechtman, Y. C. Eldar, O. Cohen, and H. N. Chapman, "Phase retrieval with application to optical imaging," *IEEE Signal Process. Mag.*, vol. 32, no. 3, pp. 87–109, May 2015.
- [18] S. S. Chen, D. L. Donoho, and M. A. Saunders, "Atomic decomposition by basis pursuit," *SIAM J. Sci. Comput.*, vol. 20, no. 1, pp. 33–61, Jan. 1998.
- [19] Y. Sun, P. Babu, and D. P. Palomar, "Majorization-minimization algorithms in signal processing, communications, and machine learning," *IEEE Trans. Signal Process.*, vol. 65, no. 3, pp. 794–816, Feb. 2017.
- [20] Q. Li, W. Liu, L. Huang, W. Sun, and P. Zhang, "An undersampled phase retrieval algorithm via gradient iteration," in *Proc. IEEE 10th Sensor Array Multichannel Signal Process. Workshop (SAM)*, Jul. 2018, pp. 228–231.
- [21] B. Amir and T. Marc, "Gradient-based algorithms with applications to signal recovery problems," in *Convex Optimization in Signal Processing and Communications*, D. P. Palomar and Y. C. Eldar, Eds. Cambridge, U.K.: Cambridge Univ. Press, 2010, pp. 42–88.
- [22] N. Parikh and S. Boyd, "Proximal algorithms," *Found. Trends Optim.*, vol. 1, no. 3, pp. 123–231, 2013.
- [23] W. Deng, W. Ying, and Y. Zhang, "Group sparse optimization by alternating direction method," Rice Univ., Houston, TX, USA, Tech. Rep. TR11-06, 2011.
- [24] M. V. W. Zibetti, E. S. Helou, R. R. Regatte, and G. T. Herman, "Monotone FISTA with variable acceleration for compressed sensing magnetic resonance imaging," *IEEE Trans. Comput. Imag.*, vol. 5, no. 1, pp. 109–119, Mar. 2019.
- [25] A. Beck and M. Teboulle, "A fast iterative shrinkage-thresholding algorithm for linear inverse problems," *SIAM J. Imag. Sci.*, vol. 2, no. 1, pp. 183–202, Jan. 2009.
- [26] Y. E. Nesterov, "A method for solving the convex programming problem with convergence rate  $O(1/k^2)$ ," *Sov. Math. Dokl.*, vol. 27, no. 2, pp. 372–376, 1983.
- [27] R. P. Balan Casazza and D. Edidin, "On signal reconstruction without phase," *Appl. Comput. Harmon. Anal.*, vol. 20, no. 3, pp. 345–356, May 2006.
- [28] A. S. Bandeira, J. Cahill, D. G. Mixon, and A. A. Nelson, "Saving phase: Injectivity and stability for phase retrieval," *Appl. Comput. Harmon. Anal.*, vol. 37, no. 1, pp. 106–125, Jul. 2014.
- [29] A. Conca, D. Edidin, M. Hering, and C. Vinzant, "An algebraic characterization of injectivity in phase retrieval," *Appl. Comput. Harmon. Anal.*, vol. 38, no. 2, pp. 346–356, Mar. 2015.
- [30] X. Li and V. Voroninski, "Sparse signal recovery from quadratic measurements via convex programming," *SIAM J. Math. Anal.*, vol. 45, no. 5, pp. 3019–3033, Jan. 2013.
- [31] H. Ohlsson and Y. C. Eldar, "On conditions for uniqueness in sparse phase retrieval," in *Proc. IEEE Int. Conf. Acoust., Speech Signal Process. (ICASSP)*, May 2014, pp. 1841–1845.
- [32] C. Qian, N. D. Sidiropoulos, K. Huang, L. Huang, and H. C. So, "Phase retrieval using feasible point pursuit: Algorithms and Cramér–Rao bound," *IEEE Trans. Signal Process.*, vol. 64, no. 20, pp. 5282–5296, Oct. 2016.
- [33] R. Balan, "Reconstruction of signals from magnitudes of redundant representations: The complex case," *Found. Comput. Math.*, vol. 16, no. 3, pp. 677–721, 2013.
- [34] S. M. Kay, *Fundamentals of Statistical Signal Processing: Estimation Theory*. Upper Saddle River, NJ, USA: Prentice-Hall, 1993.



**ZHENGYU WAN** received the B.Eng. degree in electronic information engineering from Shenzhen University, China, in 2015, and the M.Sc. degree from the Department of Electronic and Electrical Engineering, The University of Sheffield, U.K., in 2017. He is currently pursuing the Ph.D. degree with the Department of Electronic and Electrical Engineering, The University of Sheffield. His research interest includes sensor array signal processing.



**WEI LIU** (Senior Member, IEEE) received the B.Sc. and L.L.B. degrees from Peking University, China, in 1996 and 1997, respectively, the M.Phil. degree from The University of Hong Kong, Hong Kong, in 2001, and the Ph.D. degree from the School of Electronics and Computer Science, University of Southampton, U.K., in 2003.

He held a postdoctoral position first in Southampton, and later with the Department of Electrical and Electronic Engineering, Imperial College London, London. Since September 2005, he has been with the Department of Electronic and Electrical Engineering, The University of Sheffield, U.K., first as a Lecturer, and then as a Senior Lecturer. He has published more than 300 journal and conference papers, five book chapters, and two research monographs, such as *Wideband Beamforming: Concepts and Techniques*, (John Wiley, March 2010) and *Low-cost Smart Antennas* (Wiley, March 2019). His research interests include a wide range of topics in signal processing, with a focus on sensor array signal processing and its various applications, such as robotics and autonomous systems, human–computer interface, radar, sonar, satellite navigation, and wireless communications. He is a member of the Digital Signal Processing Technical Committee of the IEEE Circuits and Systems Society, where he was the Secretary, in 2020. He is also a member of the Sensor Array and Multichannel Signal Processing Technical Committee of the IEEE Signal Processing Society, where he is currently the Chair. From 2015 to 2019, he was an Associate Editor for IEEE TRANSACTIONS ON SIGNAL PROCESSING. He is also an Associate Editor of IEEE ACCESS and an Editorial Board Member of the journal *Frontiers of Information Technology and Electronic Engineering*.

...